Research Square

Preprints are preliminary reports that have not undergone peer review.
They should not be considered conclusive, used to inform clinical practice,
or referenced by the media as validated information.

Meteorological and Biometeorological Evaluation of a Population-Aware Heat Warning Framework for Mauritius

Yashvir Ramlukon

yashvir.ramlukon@gmail.com

Mauritius Meteorological Services

Research Article

Keywords:

Posted Date: November 13th, 2026

DOI: https://doi.org/10.21203/rs.3.rs-11290649/v1

License: This work is licensed under a Creative Commons Attribution 4.0 International License.
Read Full License

Additional Declarations: No competing interests reported.

Meteorological and Biometeorological Evaluation of a Population-Aware Heat Warning Framework for Mauritius

Yashvir Ramlukon

Mauritius Meteorological Services, St Paul Road, Vacoas, Republic of Mauritius

Corresponding author: yashvir.ramlukon@gmail.com

Abstract

Human biometeorological heat assessment requires metrics that distinguish local climatic rarity, multi-day persistence, nocturnal heat, combined thermal stress and spatial population exposure. We developed and evaluated a population-aware heat-warning framework for Mauritius using reference station observations, ERA5-Land reanalysis, calendar-day temperature percentiles, Excess Heat Factor (EHF), the Universal Thermal Climate Index (UTCI), nocturnal heat diagnostics and fixed-standard 2022 census weights. ERA5-Land reproduced day-to-day maximum-temperature variability but showed station-dependent cool bias (-0.28 to $-2.53^{\circ}\mathrm{C}$) and weak same-day 99th-percentile event detection. At Plaisance, derived wet-bulb temperature closely reproduced observed November–April measurements (bias $-0.076^{\circ}\mathrm{C}$; root-mean-square error $0.191^{\circ}\mathrm{C}$; $r = 0.992$). A hybrid UTCI series combining observed air temperature, humidity and wind with ERA5-Land mean radiant temperature correlated strongly with ERA5-only UTCI ($r = 0.962$) but was $2.18^{\circ}\mathrm{C}$ warmer. Historical heat episodes expressed contrasting biometeorological signatures: December 2013 combined thermal stress, EHF, hot-day and warm-night burden; February 2025 produced island-wide UTCI $\geq 38^{\circ}\mathrm{C}$ and 99th-percentile hot-day/warm-night burden without EHF severity ≥ 3; and March 2019 exposed a marked reanalysis-observation disagreement. The 1991–2025 archive contains 12,784 daily records with six-zone, island-maximum and population-fraction diagnostics. The approach provides a transferable biometeorological validation framework for data-constrained tropical islands; epidemiological calibration remains necessary before health-based alert thresholds are defined.

Keywords: human biometeorology; heat stress; Universal Thermal Climate Index; Excess Heat Factor; reanalysis validation; tropical island.

1 Introduction

Human biometeorology examines the interactions between atmospheric conditions and human thermal environments, including how temperature, humidity, radiation and wind combine to shape thermal stress. For operational heat assessment, no single index represents every relevant process. Heatwave persistence, locally unusual maximum and minimum temperatures, radiative loading and thermophysiological stress may evolve differently in time and space. This distinction is reflected in contemporary World Meteorological Organization guidance, which separates accumulated heat across successive days and nights from thermal heat stress driven by the combined effects of temperature, humidity, solar radiation and wind (World Meteorological Organization, 2026). The Global Heat Health Information Network likewise distinguishes simple temperature-based measures from more comprehensive thermal indices and emphasizes locally relevant heat characterization (Global Heat Health Information Network, 2026).

The selection and implementation of biometeorological indices therefore require explicit attention to their intended use, input data and physiological assumptions. Human heat balance depends on air temperature, mean radiant temperature, vapour pressure, air movement, metabolic heat production and clothing-related heat and moisture transfer (Havenith and Fiala, 2016). UTCI integrates several environmental drivers within a standardized thermophysiological framework (Bröde et al., 2012), whereas EHF characterizes multi-day heatwave intensity through

climatic significance and recent acclimatization (Nairn and Fawcett, 2015). Minimum-temperature percentiles provide another dimension by identifying unusually warm nights. These quantities are complementary rather than interchangeable. Recent biometeorological literature has consequently emphasized transparent reporting of index choice, data source, substitutions, assumptions and ground validation (Fitchett, 2026).

These methodological issues are particularly important on small tropical islands. Mauritius has a humid maritime tropical climate, marked topographic contrasts between coastal lowlands and the central plateau, heterogeneous urban development, and strong local modulation by elevation and sea-breeze exposure. A spatially sparse station network provides direct local measurements but cannot alone provide complete long-term environmental coverage. Reanalysis offers spatial and temporal continuity, yet may smooth local extremes. A defensible heat-warning framework therefore needs to combine observational evidence with reanalysis while retaining the distinct physical meanings of the selected heat metrics.

Population exposure adds a further spatial dimension. A high thermal-stress value confined to one representative zone does not imply the same national burden as simultaneous exceedance across several densely populated zones. At the same time, nonlinear heat-stress or heatwave categories should not be assigned to a spatially averaged index because averaging can dilute localized extremes. We therefore distinguish population-weighted continuous exposure from the fraction of a fixed-standard population represented by zones exceeding local thresholds.

The Mauritius Heat-Health Warning System (MHHWS) project is evaluated here specifically at the meteorological and biometeorological exposure stage. The aim is not to claim epidemiological validation, but to establish a reproducible heat-warning architecture that can later support health-impact calibration. The framework follows four principles: station observations are treated as the reference evidence for local historical extremes; ERA5-Land is treated as reanalysis rather than observation; percentile, persistence, nocturnal and thermophysiological pathways are retained separately; and population weighting is applied after zone-level hazard metrics are determined.

The specific objectives are to: (1) construct daily and hourly heat-exposure metrics for six representative Mauritius zones; (2) evaluate ERA5-Land against reference station observations; (3) implement and audit EHF, percentile, nocturnal heat and UTCI pathways; (4) examine historical high-severity event families; (5) quantify the population fraction represented by zones exceeding heat thresholds using final 2022 census data; and (6) create a complete 1991–2025 national exposure archive suitable for subsequent impact studies. The contribution is intended to be transferable to other data-constrained tropical islands where direct observations are spatially limited and gridded environmental products require local validation.

2 Materials and methods

2.1 Study area and six-zone exposure framework

The study domain is the Island of Mauritius. Six representative meteorological exposure strata were used to preserve broad geographical and topographic contrasts while maintaining a tractable operational framework: North (Pamplemousses), East (Fuel-East proxy), South-Southeast (Plaisance), West (Medine-West), Central Plateau (Vacoas), and Port Louis. These are representative exposure strata and should not be interpreted as formally surveyed heat-climate polygons.

For population weighting, the six strata were mapped to administrative districts through a documented district aggregation rule: Pamplemousses and Rivière du Rempart to North; Flacq to East; Grand Port and Savanne to South-Southeast; Black River to West; Plaines Wilhems and Moka to Central Plateau; and Port Louis district to Port Louis. This mapping was used solely for population exposure weighting and does not assert that district boundaries coincide with meteorological heat-zone boundaries.

Table 1: Final 2022 census population weights used for the six representative MHHWS exposure strata. The Island of Mauritius total is 1,189,493 residents.

Exposure stratum	Population	Weight	District aggregation
Central Plateau	426,318	0.358403	Plaines Wilhems + Moka
North	252,051	0.211898	Pamplemousses + Rivière du Rempart
South-Southeast	178,562	0.150116	Grand Port + Savanne
East	138,529	0.116461	Flacq
Port Louis	106,332	0.089393	Port Louis
West	87,701	0.073730	Black River
Total	1,189,493	1.000000	Island of Mauritius

Final census Table G1 reports an Island of Mauritius resident population of 1,189,493 (Statistics Mauritius, 2022). The weights in Table 1 are therefore based on the final geographical table rather than the earlier preliminary census headline totals.

2.2 Meteorological datasets

2.2.1 ERA5-Land

ERA5-Land was used as the spatially complete environmental reconstruction for the six representative points. ERA5-Land provides hourly land-surface fields at high spatial resolution and is forced by ERA5 atmospheric fields; it does not directly assimilate surface observations in the same way as a station dataset (Muñoz-Sabater et al., 2021). The analysis used 1991–2025 as the main historical period, with 1991–2020 as the climatological baseline for calendar-day percentiles and heatwave normalization.

Daily maximum temperature ($T_{\max}$), minimum temperature ($T_{\min}$) and mean temperature (T_{mean}) were derived from the hourly fields. Radiation, humidity and wind were used for mean radiant temperature (MRT) and UTCI calculations. A critical radiation-processing correction was implemented during development: ERA5-Land accumulated radiation valid at time T was interpreted as representing the preceding interval $[T - 1\mathrm{h}, T]$. The MRT calculation therefore used $T - 1\mathrm{h}$ as the radiation interval start while retaining T as the output valid time. This correction removed physically implausible nocturnal MRT artifacts.

2.2.2 Daily station observations

Reference daily maximum-temperature observations were available from the project archive for Pamplemousses, Fuel, Medine, Plaisance and Vacoas. Port Louis was not available in the same archive. These observations were used to evaluate ERA5-Land daily maximum temperature and percentile-exceedance behaviour.

GHCN-Daily data were used where appropriate for independent or supplementary station series. GHCN-Daily is a quality-controlled global station database designed for daily climate analysis (Menne, Durre, et al., 2012). For Plaisance and Vacoas, GHCN daily series were recognized as sharing station lineage with parts of the local archive; they were therefore treated as consistency/supplementary evidence rather than automatically as statistically independent validation.

2.2.3 Hourly Plaisance observations

Hourly Plaisance temperature, relative humidity, wet-bulb temperature and wind were obtained from the NOAA Global Historical Climatology Network-Hourly (GHCNh), which supersedes the legacy Integrated Surface Dataset and harmonizes multiple source streams (Menne, Noone, et al., 2023). Hourly temperature was also compared against

ISD for lineage consistency; the near-identical series demonstrated that the two should not be counted as independent datasets.

2.3 Validation statistics and computational workflow

Continuous-variable evaluation used mean bias, mean absolute error (MAE), root-mean-square error (RMSE) and Pearson correlation. Extreme-event skill used probability of detection (POD), false-alarm ratio (FAR) and critical success index (CSI). Analyses were implemented in Python 3.12 under Ubuntu 24.04 and were frozen with SHA256 manifests before health-model development. ChatGPT (OpenAI) assisted with code/document drafting and consistency checking; the author executed the analyses, inspected outputs, verified numerical results against project logs and source data, and takes responsibility for the final methods and interpretation.

2.4 Calendar-day percentile climatology

Calendar-day thresholds were computed using 1991–2020 and a ± 15-day moving window around each calendar day. Thresholds included TX90, TX95 and TX99 for daily maximum temperature and TN90, TN95 and TN99 for daily minimum temperature. The principal warm season was November–April.

Percentile exceedances were treated as local relative-extreme indicators, not as direct health thresholds. This local-threshold approach is consistent with WMO guidance that heatwaves should generally be defined relative to local climatic conditions rather than by a universal absolute temperature (World Meteorological Organization, 2026). Because a percentile definition adapts to local climatology, a percentile exceedance at a cooler high-elevation station does not imply the same absolute physiological stress as the same percentile at a warmer coastal station.

2.5 Excess Heat Factor

The EHF framework followed the acclimatization and significance structure introduced by Nairn and Fawcett (2015). Let

$$T_3(d) = \frac{1}{3}\sum_{i=0}^{2} T_{\mathrm{mean}}(d+i), \tag{1}$$

with the previous 30-day mean

$$T_{30}(d) = \frac{1}{30}\sum_{i=1}^{30} T_{\mathrm{mean}}(d-i). \tag{2}$$

The heat-significance and acclimatization terms were

$$EHI_{\mathrm{sig}}(d) = T_3(d) - T_{95}(d), \tag{3}$$

$$EHI_{\mathrm{accl}}(d) = T_3(d) - T_{30}(d), \tag{4}$$

where $T_{95}(d)$ is the local calendar-day 95th percentile of daily mean temperature. EHF was then calculated as

$$EHF(d) = EHI_{\mathrm{sig}}(d)\max\left(1, EHI_{\mathrm{accl}}(d)\right). \tag{5}$$

A local severity index was computed as

$$S_{EHF} = \frac{EHF}{EHF_{85}}, \tag{6}$$

where EHF_{85} is the 85th percentile of positive baseline EHF. The project classification was: $S_{EHF} \leq 0$ no EHF heatwave signal; $0 < S_{EHF} < 1$ low; $1 \leq S_{EHF} < 3$ severe; and $S_{EHF} \geq 3$ extreme.

Because this formulation uses a forward three-day mean, strict observational EHF beginning on day d requires a continuous 33-day T_{mean} sequence (30 antecedent days plus $d, d+1, d+2$). This requirement was enforced in the

observational audit; missing observations were not interpolated merely to manufacture EHF continuity.

2.6 UTCI, MRT and heat-stress classes

UTCI represents the thermal environment through an equivalent temperature based on modeled human thermophysiological response to air temperature, humidity, wind and mean radiant temperature (Bröde et al., 2012). In the broader heat-balance literature, UTCI is distinguished from simpler empirical indices because it is based on physiological simulation and was designed for biometeorological weather services and epidemiological applications (Havenith and Fiala, 2016). Its inclusion is also consistent with the WMO distinction between heatwave magnitude and human thermal heat stress, for which temperature alone is insufficient because humidity, radiation and wind materially affect physiological strain (World Meteorological Organization, 2026). The project used the standard heat-stress categories: moderate heat stress at $26 \leq UTCI < 32^{\circ}\mathrm{C}$, strong heat stress at $32 \leq UTCI < 38^{\circ}\mathrm{C}$, very strong heat stress at $38 \leq UTCI < 46^{\circ}\mathrm{C}$, and extreme heat stress at $UTCI \geq 46^{\circ}\mathrm{C}$.

UTCI is nevertheless not interpreted here as a direct health-risk model for all members of the Mauritius population. Its physiological reference representation is standardized, whereas susceptibility to heat varies with age, pregnancy, chronic disease, activity, clothing, acclimatization and other individual factors. Recent commentary specifically notes that even physiologically based indices such as UTCI can under-represent the responses of vulnerable groups if their standard reference assumptions are transferred directly to population-health risk categories (Jay and Jahan, 2026). Accordingly, UTCI in the MHHWS is treated as one biometeorological exposure pathway that requires local health-outcome calibration rather than as an intrinsically health-validated warning scale.

UTCI calculations were implemented using `pythermalcomfort` (Tartarini and Schiavon, 2020); climate-processing utilities included `xclim` (Bourgault et al., 2023). The final corrected ERA5-Land UTCI archive contained 1,840,452 valid UTCI hours across the six points. Maximum UTCI values by point ranged from $39.51^{\circ}\mathrm{C}$ at Plaisance to $40.76^{\circ}\mathrm{C}$ at Medine-West.

The UTCI wind application domain was respected: observed wind below $0.5\mathrm{m\,s^{-1}}$ was mapped to $0.5\mathrm{m\,s^{-1}}$, whereas values above $17\mathrm{m\,s^{-1}}$ were not clipped downward; hybrid UTCI was left missing for such hours. The measurement height/exposure of the GHCNh wind series remains unverified, so the hybrid UTCI analysis is interpreted as a sensitivity/validation experiment rather than a fully observation-constrained operational product.

2.7 Wet-bulb validation at Plaisance

A continuous derived wet-bulb series was calculated from air temperature and relative humidity using the Stull (2011) approximation and compared with available observed wet-bulb temperatures. The observed wet-bulb archive contained 2,341 values over 177 days from 1973 to 2026. Validation was emphasized for the warm season and heat-relevant conditions.

2.8 Fit-for-purpose interpretation of heat metrics

The framework intentionally avoids treating the available heat metrics as interchangeable. GHHIN distinguishes simple temperature-humidity indices from more complex thermal indices that incorporate radiation and wind, and emphasizes that HHWS thresholds should be locally relevant and connected to health impacts (Global Heat Health Information Network, 2026). The thermophysiological literature likewise shows that different indices encode different components of human-environment heat exchange and were developed for different contexts (Havenith and Fiala, 2016). The interpretation adopted here is summarized in Table 2.

Table 2: Fit-for-purpose interpretation of the principal MHHWS exposure metrics.

Metric family	Primary interpretation in this study	What it does not establish by itself
TX/TN percentiles	Local climatological rarity of hot days and warm nights	Absolute physiological strain or health risk
EHF	Multi-day heatwave intensity incorporating recent acclimatization and climatological significance	Individual thermal strain or cause-specific morbidity
UTCI	Modeled outdoor thermal stress integrating temperature, humidity, wind and MRT for a standardized physiological reference	Population-specific health risk in vulnerable groups without epidemiological validation
Population fraction above threshold	Spatial burden under the fixed 2022 population standard while preserving zone-level nonlinear criteria	Individual exposure, attributable illness or mortality
Station observations	Local measured meteorological evidence at available stations	Complete island-wide spatial exposure
ERA5-Land	Spatially and temporally complete reanalysis-based environmental reconstruction	A substitute for station observations at local extremes

This separation follows the broader methodological principle that metric origin, input fidelity and target population should remain explicit. In particular, a reconstructed or hybrid quantity should be labelled as such, and population-health warning thresholds should be validated against the population to which they will be applied (Jay and Jahan, 2026).

2.9 Historical warning architecture

An early historical warning matrix (v0.5.1) used independent local pathways:

- Yellow: $S_{EHF} \geq 1$ or TN90 for at least 3 nights;
- Orange: $S_{EHF} \geq 2$, or TN95 for at least 5 nights, or concurrent TX95 and TN95 for at least 3 days;
- Red candidate: $S_{EHF} \geq 3$, or TN99 for at least 5 nights, or concurrent TX99 and TN99 for at least 2 days.

A later reanalysis research candidate (v1.2) strengthened Red logic by adding UTCI support to percentile-based Red pathways while retaining EHF severity ≥ 3 as an independent Red mechanism. It reduced the number of reanalysis Red days from 17 to 8. This version was never treated as operationally health-validated.

The subsequent v1.8.2 and v1.9 evidence matrices did not simply replace one warning algorithm with another. Instead, they integrated reference observed TX/TN evidence and Plaisance hybrid UTCI evidence to determine whether reanalysis-based historical classifications were supported, contradicted, or unresolved.

2.10 Population exposure burden

For a threshold criterion C and date d, the population fraction exposed was defined as

$$F_C(d) = \frac{\sum_{z \in V_d} w_z I\{C_z(d) = 1\}}{\sum_{z \in V_d} w_z}, \tag{7}$$

where w_z is the fixed 2022 population weight of zone z, V_d is the set of zones with valid data on day d, and I is the indicator function. This approach preserves zone-level nonlinear threshold logic. It differs fundamentally from applying a UTCI or EHF category to a population-weighted mean.

Daily population fractions were calculated for UTCI ≥ 32, ≥ 38 and $\geq 46^{\circ}\mathrm{C}$; EHF severity ≥ 1 and ≥ 3; TX90/TX95/TX99; and TN90/TN95/TN99. Population-weighted mean exposure and island-maximum exposure were retained as separate continuous descriptors.

2.11 Daily national exposure archive

The final daily exposure dataset was restricted to complete calendar years, 1 January 1991 through 31 December 2025, producing 12,784 daily records. It contains 17 primary exposure variables plus lag 1–7 values and 3-day/7-day moving summaries. Population weights are explicitly labelled as `FIXED_2022_STANDARD_POPULATION`. A frozen pre-health snapshot with SHA256 checksums was created so later health-model experimentation cannot silently modify the meteorological evidence base.

No real aggregated morbidity or mortality dataset was available at the time of this study. Health-calibration scripts therefore contain explicit stop conditions for empty templates, direct identifiers, invalid/negative counts, duplicate date-geography records and inappropriate national/local geographic merging.

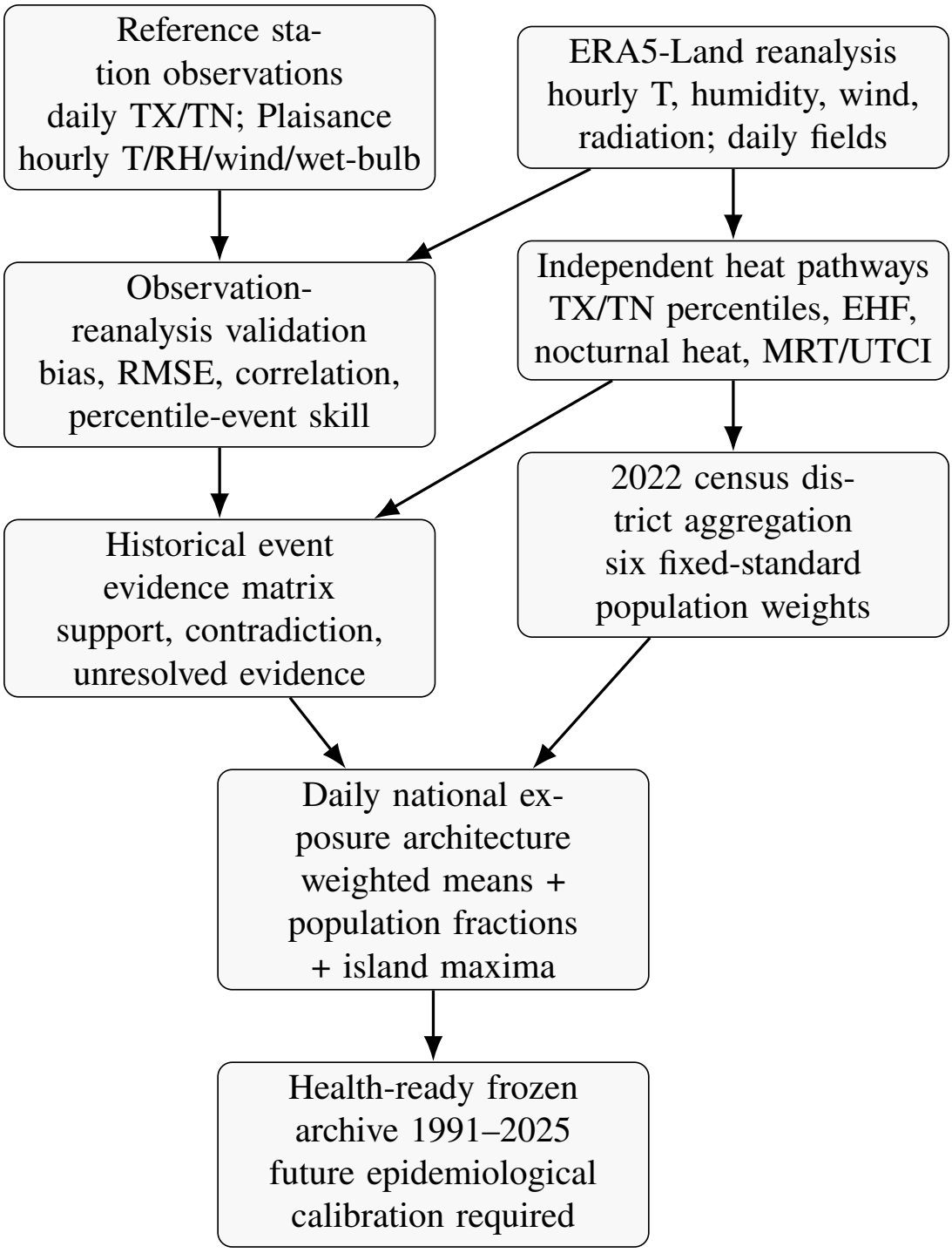


Figure 1: Conceptual workflow of the MHHWS pre-health-calibration architecture. Reanalysis provides spatial and temporal completeness; station observations constrain historical event evidence; population burden is calculated only after zone-level hazard metrics have been determined.

3 Results

3.1 Historical warning-day sensitivity to Red-definition changes

Across 6,163 November–April days in 1991–2025, v0.5.1 produced 5,694 Green, 365 Yellow, 87 Orange and 17 Red national days. The stricter v1.2 reanalysis research architecture retained the same Green and Yellow counts

but redistributed high-end severity to 96 Orange and 8 Red days. The original Red-containing event families were February 2004, December 2013, March 2019, November 2023, January 2024, February 2025, 13–15 April 2025 and 24–28 April 2025. Under v1.2, the 2004, 2013, November 2023, January 2024 and February 2025 families retained Red days, while the March 2019 and two April 2025 families were downgraded.

This reduction demonstrated high sensitivity of the most severe category to the addition of UTCI and nocturnal support. It also motivated the subsequent observational audit: a reanalysis algorithm that suppresses a historical Red signal cannot be considered validated merely because its internal criteria are more restrictive.

3.2 ERA5-Land daily maximum temperature validation

ERA5-Land reproduced daily temperature variability with high correlations but systematic station-dependent cool bias (Table 3; Fig. 2). Biases were most pronounced at lowland stations and smallest at Vacoas. The observed station relationships demonstrate that a single island-wide additive bias correction would be physically inappropriate.

Table 3: ERA5-Land daily maximum temperature validation against reference station observations. Bias is ERA5-Land minus observed. Correlation confidence intervals use the Fisher z approximation.

Station	Paired days	Bias (°C)	r	95% CI	TX99 POD	TX99 CSI
Fuel	12,120	-1.458	0.906	0.903–0.909	0.051	0.029
Medine	12,016	-2.267	0.854	0.849–0.859	0.074	0.048
Pamplemousses	5,916	-2.533	0.910	0.906–0.914	–	–
Plaisance	12,144	-1.888	0.932	0.930–0.934	0.237	0.140
Vacoas	12,097	-0.275	0.932	0.930–0.934	0.100	0.057

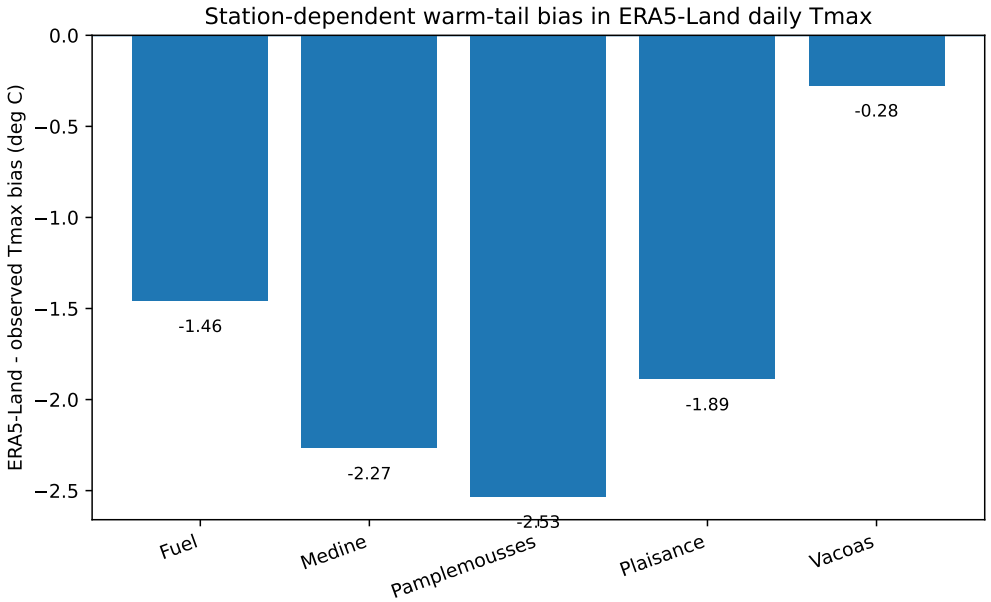


Figure 2: ERA5-Land minus observed daily maximum-temperature bias. The strong spatial variation in bias is evidence against applying one island-wide additive correction.

Same-day TX99 detection was poor even where continuous temperature correlation was high. Timing tolerances of one or two days improved event correspondence only modestly. Thus ERA5-Land was retained for climatological reconstruction, spatial completeness and environmental context, but reference station observations were given higher evidential priority for historical local extremes.

3.3 Observed minimum-temperature and strict EHF limitations

At Plaisance, ERA5-Land minus observed $T_{\min}$ bias was approximately $+0.39^{\circ}\mathrm{C}$ (RMSE $1.17^{\circ}\mathrm{C}$, correlation 0.893), with observed and ERA5-Land p99 values of 25.6 and $25.27^{\circ}\mathrm{C}$, respectively. At Vacoas, the corresponding bias was $+1.63^{\circ}\mathrm{C}$ (RMSE $1.90^{\circ}\mathrm{C}$, correlation 0.925), with observed and ERA5-Land p99 values of 23.1 and $24.23^{\circ}\mathrm{C}$.

Gap-aware TN99 skill remained modest: at Plaisance POD was 0.100, FAR 0.889 and CSI 0.056; at Vacoas POD was 0.256, FAR 0.725 and CSI 0.153. For TN95 persistence of at least five nights, Plaisance had 11 observed runs and 17 ERA5-Land runs with zero matched hits, while Vacoas had 21 observed runs, 36 ERA5-Land runs and 14 hits (POD 0.667; FAR 0.611; CSI 0.326).

Strict observational EHF was strongly constrained by missing daily minima. During 1991–2020, Plaisance had approximately 43.6% strict-EHF availability and Vacoas only 1.6%. None of the eight historical Red-family windows had a complete strict observational EHF sequence at either station. Missingness was therefore treated as unknown and as a break in persistence; it was not converted to a negative event and was not interpolated for the purpose of claiming EHF validation.

3.4 Plaisance wet-bulb and hourly-extreme evaluation

Derived wet-bulb temperature closely reproduced the observed Plaisance wet-bulb measurements. For all 2,341 paired values, the bias was $-0.160^{\circ}\mathrm{C}$, MAE $0.195^{\circ}\mathrm{C}$, RMSE $0.238^{\circ}\mathrm{C}$ and correlation 0.997. During November–April ($n = 897$), performance improved to bias $-0.076^{\circ}\mathrm{C}$, MAE $0.142^{\circ}\mathrm{C}$, RMSE $0.191^{\circ}\mathrm{C}$ and correlation 0.992. Under heat-relevant conditions ($T \geq 26.7^{\circ}\mathrm{C}$ and RH $\geq 60\%$), the derived series retained RMSE near $0.19^{\circ}\mathrm{C}$ and correlation about 0.99.

Hourly temperature sampling did not perfectly recover official daily extrema. On days with at least 18 hourly observations, hourly maximum temperature was biased low by $0.469^{\circ}\mathrm{C}$ and hourly minimum temperature was biased high by $0.476^{\circ}\mathrm{C}$. Consequently, hourly GHCNh temperature was not substituted for official daily TX/TN in the historical percentile validation.

3.5 Observed wind and hybrid UTCI

A total of 274,122 paired Plaisance wind observations were compared with ERA5-Land. ERA5-Land wind was stronger on average by $1.077\,\mathrm{m\,s^{-1}}$ (MAE $1.511\,\mathrm{m\,s^{-1}}$, RMSE $1.904\,\mathrm{m\,s^{-1}}$, correlation 0.736). The observed mean was $4.240\,\mathrm{m\,s^{-1}}$ and p95 $7.7\,\mathrm{m\,s^{-1}}$, compared with an ERA5-Land mean of $5.317\,\mathrm{m\,s^{-1}}$ and p95 $8.987\,\mathrm{m\,s^{-1}}$.

The hybrid UTCI series combined observed Plaisance air temperature, relative humidity and wind with ERA5-Land MRT. It contained 270,402 valid values. Relative to ERA5-only UTCI, hybrid UTCI had bias $+2.175^{\circ}\mathrm{C}$, MAE $2.417^{\circ}\mathrm{C}$, RMSE $2.788^{\circ}\mathrm{C}$ and correlation 0.962. The hybrid p95 was $33.827^{\circ}\mathrm{C}$, p99 $36.039^{\circ}\mathrm{C}$, and maximum $41.153^{\circ}\mathrm{C}$; 334 hours reached at least $38^{\circ}\mathrm{C}$, while none reached $46^{\circ}\mathrm{C}$.

December 2013, January 2024 and February 2025 reached or exceeded the local 1991–2020 warm-season p99 of daily hybrid UTCI maxima; February 2004 exceeded $38^{\circ}\mathrm{C}$ but was below the p99. March 2019, November 2023 and the April 2025 events showed comparatively limited Plaisance UTCI support. Importantly, no event had nocturnal UTCI $\geq 32^{\circ}\mathrm{C}$, demonstrating that warm-night percentile burden and nocturnal UTCI represent different physical/physiological constructs and should not be collapsed into a single pathway.

3.6 Integrated historical event evidence

The evidence integration altered interpretation without automatically reclassifying historical warnings. February 2004 had strong persistent observed TX99 evidence and limited TN support, with EHF severity supporting a persistent heatwave pathway. December 2013 had moderate observed extreme-temperature evidence, limited TN99 support and strong daytime physiological support. March 2019 had the strongest conflict between reanalysis and observations: reference station data indicated a strong multizone extreme episode, while v1.2 downgraded the event. The later

evidence matrix therefore classified March 2019 as a Red-reconsideration case rather than accepting the reanalysis downgrade as definitive.

November 2023 had moderate observed TX evidence but limited Plaisance UTCI and no TN99 at the two GHCN validation stations; this did not disprove the northern-zone signal because the absence of extreme minima at Plaisance and Vacoas is not island-wide negative evidence. January 2024 had moderate observed TX and TN support plus strong Plaisance daytime physiological support. February 2025 lacked the original multi-station `AllTemp` archive after March 2024, but later Plaisance GHCN data provided supplementary local TX/TN and UTCI evidence. The two April 2025 event families remained less strongly supported physiologically at Plaisance and lacked complete original multi-station observational coverage.

3.7 Population exposure climatology

The 1991–2020 November–April population-exposure climatology showed that national mean and island-maximum metrics have different distributions. Population-weighted UTCI maxima had a p99 of $37.27^{\circ}\mathrm{C}$, while the island maximum had a p99 of $38.85^{\circ}\mathrm{C}$. Population-weighted EHF severity had a p99 of 1.045, whereas island-maximum EHF severity had a p99 of 1.623 and a baseline maximum of 4.263.

The population-fraction diagnostics demonstrate why weighted nonlinear indices should not be categorized directly. The population-weighted EHF maximum over the full daily archive was 2.962, below the local extreme threshold of 3, yet individual zones reached severity above 3 and up to 41.8% of the fixed-standard population was simultaneously represented by such zones. Averaging a nonlinear severity index therefore dilutes localized extremes.

3.8 Population-burden crosswalk of historical Red-family events

Figure 3 shows the multi-pathway nature of historical heat. December 2013 reached a maximum population fraction of 0.570 above UTCI $\geq 38^{\circ}\mathrm{C}$, 0.418 above EHF severity ≥ 3, 0.850 in TX99 zones and 1.000 in TN99 zones. February 2025 reached 1.000 for UTCI $\geq 38^{\circ}\mathrm{C}$, TX99 and TN99, but no zone reached EHF severity ≥ 3. February 2004 exhibited the converse pattern: no zone reached UTCI $\geq 38^{\circ}\mathrm{C}$ in the ERA5-based six-zone reconstruction, but the island maximum EHF severity reached 4.263, 15.0% of the population was represented by EHF-severity-≥ 3 zones, and TN99 burden reached 1.000.

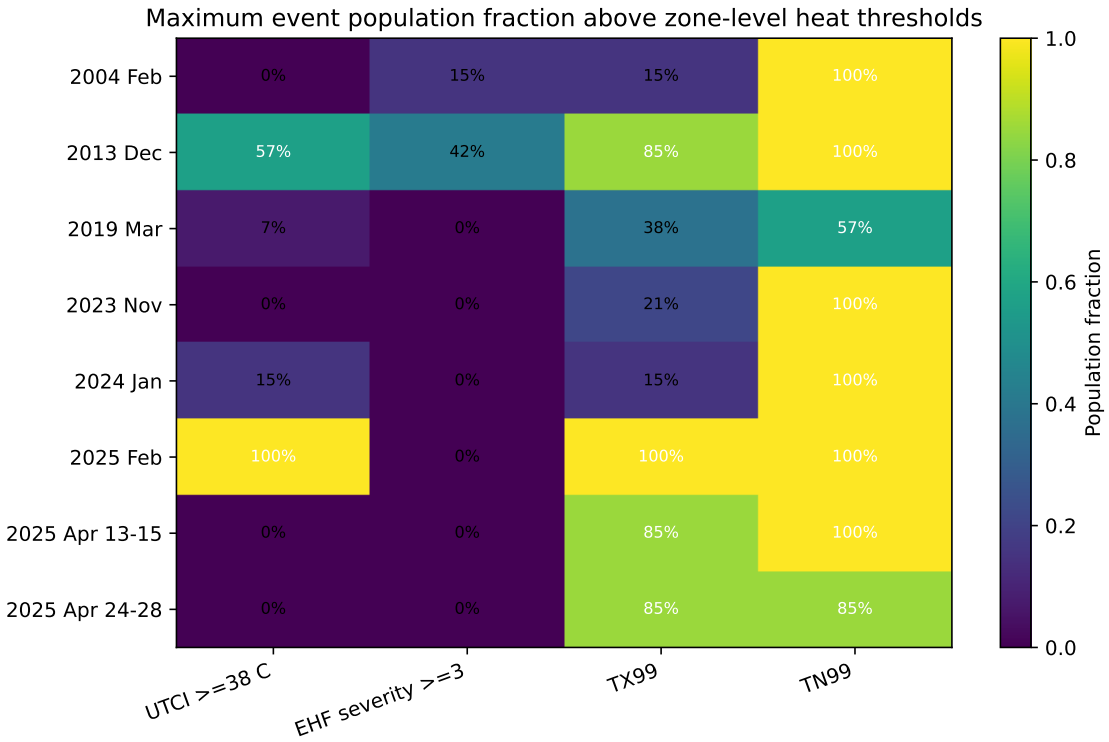


Figure 3: Maximum population fraction represented by zones exceeding four independent heat criteria during each historical event. The contrasting patterns show that daytime physiological stress, heatwave acclimatization/persistence, hot-day extremes and warm-night extremes identify different dimensions of hazard.

The March 2019 event is the clearest warning against interpreting weak reanalysis burden as proof of weak historical heat. Its ERA5-derived population fractions were only 0.074 for UTCI $\geq 38°\mathrm{C}$, 0 for EHF severity ≥ 3, 0.375 for TX99 and 0.568 for TN99, yet reference observations showed a strong multizone extreme episode. This discrepancy is scientifically useful: it quantifies a failure mode of the reconstruction and justifies retaining observation-first historical evidence.

The April 2025 events show another limitation of percentile-only criteria. Both windows reached population fractions near 0.85 for TX99 and 0.85–1.00 for TN99, while UTCI $\geq 38°\mathrm{C}$ and EHF severity ≥ 3 were absent. Such patterns support maintaining independent pathways and avoiding automatic Red classification solely from relative percentiles, especially late in the warm season.

3.9 Daily exposure archive and reproducibility freeze

The final national exposure table contains 12,784 rows from 1 January 1991 to 31 December 2025 with no missing dates and no duplicate dates. Population-weighted $T_{\max}$ and $T_{\min}$ are complete. There is one missing day in UTCI maxima, six in population-weighted dark-night UTCI, and 33 in EHF severity, consistent with source/algorithm availability rather than silent imputation.

The dataset contains continuous exposure variables, population fractions, island maxima, lag 1–7 variables and 3-day/7-day moving summaries. A pre-health snapshot copied 14 authoritative exposure, weighting, QC and methodology files and generated SHA256 hashes. The external compressed archive was subsequently verified using `sha256sum`. The health-data audit found zero scientifically usable real aggregated health-outcome files; all candidate project health tables were empty templates or framework files.

4 Discussion

4.1 Multi-pathway interpretation and alignment with heat-health guidance

The central result is not a single "best" heat index. EHF represents persistence and acclimatization, TX/TN percentiles identify local relative extremes, UTCI represents combined thermal stress from temperature, humidity, radiation and wind, nocturnal metrics describe overnight relief, and population fractions quantify spatial burden. Their divergence across historical events shows why averaging these pathways into one score can conceal physically important extremes.

This layered design is consistent with WMO guidance that no single metric captures all dimensions of extreme heat and that heatwave accumulation across successive days and nights is distinct from instantaneous thermal heat stress (World Meteorological Organization, 2026). It also follows GHHIN guidance that heat-health warning systems should use locally relevant thresholds and connect meteorological conditions to health impacts (Global Heat Health Information Network, 2026). Population fractions are therefore an exposure bridge between hazard detection and later impact-based decisions, not estimates of morbidity or mortality.

4.2 Observation-reanalysis complementarity

ERA5-Land provides the spatial completeness required for a long exposure archive, but high correlation did not guarantee reliable representation of the hot tail. Station-dependent cool biases, weak same-day TX99 skill and the March 2019 discrepancy demonstrate why reanalysis-only severe-warning logic can understate an observed event. A single island-wide bias correction is not supported by the station results. Future operations should prioritize direct station monitoring and, where model adjustment is needed, calibrate it locally and verify it independently.

4.3 Biometeorological and population interpretation

Warm-night percentiles and UTCI are complementary. TN99 identifies nights that are unusually warm relative to local climatology even when nocturnal UTCI remains below the standard strong-heat-stress category; conversely, daytime UTCI may increase through radiation and weak wind without an equally extreme temperature percentile. Hybrid Plaisance UTCI is useful sensitivity evidence because observed temperature, relative humidity and wind replace three reanalysis inputs, but it remains partly reconstructed because MRT is ERA5-Land-derived and wind exposure/height is unverified.

Population fractions preserve zone-level nonlinear criteria and answer a national exposure question more directly than categorizing a spatial mean. The fixed 2022 census weights are a standardization, not a reconstruction of historical population geography. A future GIS implementation should use formal meteorological heat-zone polygons or a gridded population surface if these become available.

4.4 Operational interpretation, transferability and future impact calibration

The study intentionally separates biometeorological evaluation from health-outcome calibration. WMO/WHO and GHHIN guidance treats health-based HHWS threshold setting as a meteorological-epidemiological and public-health task (World Meteorological Organization and World Health Organization, 2015; Global Heat Health Information Network, 2026). This boundary also addresses the "metric migration" problem: composite indices should retain transparent calibration context, input fidelity and population-relevant validation (Jay and Jahan, 2026). The MHHWS therefore labels ERA5-Land and hybrid quantities explicitly and treats UTCI as a biometeorological exposure metric rather than a Mauritius-specific clinical risk scale.

If real aggregated daily health outcomes become available, the frozen exposure archive can support lagged and nonlinear count models, including distributed-lag analyses (Gasparrini et al., 2010; Gasparrini, 2011). Candidate alert thresholds should then be assessed against health risk, false-alarm burden, lead time, spatial coverage and

operational feasibility. Until that stage, the framework is appropriate for retrospective event evaluation and preparation of operational procedures, not for declaring any UTCI or percentile value intrinsically "Red" for Mauritius.

The transferable contribution is the biometeorological validation sequence: local station observations constrain extremes; reanalysis supplies environmental completeness; local percentile/persistence and thermophysiological metrics remain distinct; population burden is calculated after zone-level hazard classification; and impact calibration can follow as a separate stage. Numerical thresholds, reanalysis bias, population geography and vulnerability must be recalibrated locally rather than exported from Mauritius.

4.5 Limitations

Several limitations must be retained in any interpretation or publication of this work.

1. **Incomplete observational coverage.** Reference daily $T_{\min}$ is not continuous enough to validate strict EHF for historical Red-family events, and the original multi-station daily archive ends before most 2025 events.

2. **Station lineage.** GHCN and local archives at Plaisance/Vacoas share underlying station lineage; GHCNh and legacy ISD temperature at Plaisance are also largely the same observational lineage. These checks demonstrate consistency, not independent replication.

3. **Reanalysis bias.** ERA5-Land underestimates hot daily maxima at several lowland stations and has limited TX99 event skill.

4. **Hybrid UTCI.** Plaisance UTCI is not fully observed because MRT is reanalysis-derived and wind height/exposure is unverified.

5. **Thermal-index transferability.** UTCI is a physiologically based environmental index, not a Mauritius-specific clinical risk model. Its standardized reference-person assumptions may not represent older adults, pregnant people, persons with chronic disease or other vulnerable groups; direct population-health interpretation therefore requires local outcome validation (Jay and Jahan, 2026).

6. **Six-zone discretization.** Population burden is calculated from six representative strata, not a continuous human-exposure surface.

7. **Fixed census weights.** The 2022 weights standardize 1991–2025 exposure but do not reconstruct historical population distributions.

8. **No health-outcome calibration.** No morbidity or mortality series was available. The present warning levels are therefore meteorological and biometeorological research candidates rather than health-validated thresholds.

9. **No causal health inference.** The population fractions quantify meteorological exposure burden only; they are not estimates of illness, mortality or attributable risk.

5 Conclusions

A reproducible, population-aware heat-warning framework for Mauritius has been developed and evaluated over 1991–2025 using complementary meteorological and human-biometeorological metrics. Six conclusions emerge.

First, ERA5-Land is valuable for spatially complete climatology and environmental reconstruction but does not reproduce local hot extremes sufficiently well to replace reference station observations. Second, heat severity in Mauritius is intrinsically multi-dimensional: EHF, hot-day percentiles, warm-night percentiles and UTCI identify complementary processes rather than interchangeable measures. Third, physically correct radiation timing and observed-wind sensitivity materially improve the credibility of MRT/UTCI calculations. Fourth, population fractions above zone-level thresholds retain local nonlinear criteria and are more informative for spatial burden than categorizing

population-weighted nonlinear indices. Fifth, the March 2019 event demonstrates why reanalysis-derived severe-event classifications should be checked against observed evidence. Sixth, the resulting 12,784-day exposure archive provides a stable basis for future operational evaluation and impact studies.

The framework should therefore be interpreted as a meteorologically and biometeorologically evaluated heat-warning architecture, not as a completed clinical risk model. Its multi-pathway structure is consistent with the WMO distinction between persistent heatwaves and instantaneous thermal heat stress (World Meteorological Organization, 2026) and with current biometeorological emphasis on transparent index selection, input fidelity and ground validation (Fitchett, 2026). Numerical thresholds, reanalysis bias, population geography and vulnerability should be recalibrated locally when the approach is transferred to other settings. For Mauritius, future epidemiological linkage can test whether any of the meteorological and biometeorological pathways provide additional predictive value for morbidity or mortality, but that subsequent stage is not required to establish the exposure-validation findings reported here.

Statements and Declarations

Funding No funding was received for conducting this study.

Competing interests The author declares no competing financial or non-financial interests.

Ethics approval Not applicable. The study used meteorological, reanalysis and aggregated census information and did not involve human participants or individual-level health records.

Consent to participate and consent for publication Not applicable.

Data availability ERA5-Land is available through the Copernicus Climate Data Store; GHCN products are available through NOAA/NCEI; and final 2022 census tables are available from Statistics Mauritius. Local station observations used for validation are institutional holdings and are subject to Mauritius Meteorological Services permissions. Redistributable derived products may be requested from the corresponding author, subject to those institutional conditions and third-party data licences.

Code availability The workflow was developed in Python 3.12 under Ubuntu 24.04 using numbered, phase-based scripts. Redistributable analysis code may be requested from the corresponding author; any release will exclude restricted observational data, credentials and material whose redistribution is not authorized.

Use of generative AI and AI-assisted technologies ChatGPT (OpenAI) assisted with code/document drafting, organization, language editing and consistency checking. The author executed and verified the analyses, reviewed all generated material and takes full responsibility for the manuscript, methods, results and conclusions.

Acknowledgements The author acknowledges the European Centre for Medium-Range Weather Forecasts/Copernicus Climate Change Service for ERA5-Land, NOAA National Centers for Environmental Information for GHCN products, Statistics Mauritius for the 2022 Population Census, and the Mauritius Meteorological Services for the institutional context and local observational resources used in developing the framework.

References

Bourgault, P., D. Huard, T. J. Smith, T. Logan, A. Aoun, J. Lavoie, É. Dupuis, G. Rondeau-Genesse, R. Alegre, C. Barnes, A. Beaupré Laperrière, S. Biner, D. Caron, C. Ehbrecht, J. Fyke, T. Keel, M.-P. Labonté, L. Lierhammer, J.-F. Low, J. Quinn, P. Roy, D. Squire, A. Stephens, M. Tanguy, and C. Whelan (2023). xclim: xarray-based climate data analytics. *Journal of Open Source Software* 8.85, p. 5415. https://doi.org/10.21105/joss.05415.

Bröde, P., D. Fiala, K. Błażejczyk, I. Holmér, G. Jendritzky, B. Kampmann, B. Tinz, and G. Havenith (2012). Deriving the Operational Procedure for the Universal Thermal Climate Index (UTCI). *International Journal of Biometeorology* 56.3, pp. 481–494. https://doi.org/10.1007/s00484-011-0454-1.

Fitchett, J. M. (2026). Critical Engagement on the Selection and Reporting of Biometeorological Indices. *International Journal of Biometeorology* 70, p. 261. https://doi.org/10.1007/s00484-026-03328-9.

Gasparrini, A. (2011). Distributed Lag Linear and Non-Linear Models in R: The Package dlnm. *Journal of Statistical Software* 43.8, pp. 1–20. https://doi.org/10.18637/jss.v043.i08.

Gasparrini, A., B. Armstrong, and M. G. Kenward (2010). Distributed Lag Non-linear Models. *Statistics in Medicine* 29.21, pp. 2224–2234. https://doi.org/10.1002/sim.3940.

Global Heat Health Information Network (2026). *Understanding Heat: From Urban Heat Islands to Heatwaves*. Overview of heat indices, heatwave characterization, monitoring and heat-health warning systems. URL: `https://heathealth.info/understanding-heat/` (visited on 09/24/2026).

Havenith, G. and D. Fiala (2016). Thermal Indices and Thermophysiological Modeling for Heat Stress. *Comprehensive Physiology* 6.1, pp. 255–302. https://doi.org/10.1002/cphy.c140051.

Jay, O. and F. Jahan (2026). The Science of Climate Heat Risks Has a Metric Problem. *Communications Earth & Environment* 7. Comment, p. 595. https://doi.org/10.1038/s43247-026-03804-5.

Menne, M. J., I. Durre, R. S. Vose, B. E. Gleason, and T. G. Houston (2012). An Overview of the Global Historical Climatology Network-Daily Database. *Journal of Atmospheric and Oceanic Technology* 29.7, pp. 897–910. https://doi.org/10.1175/JTECH-D-11-00103.1.

Menne, M. J., S. Noone, N. W. Casey, R. H. Dunn, S. McNeill, D. Kantor, P. W. Thorne, K. Orcutt, S. Cunningham, and N. Risavi (2023). *Global Historical Climatology Network-Hourly (GHCNh)*. NOAA National Centers for Environmental Information. Subset used for Plaisance and Vacoas observational evaluation. https://doi.org/10.25921/jp3d-3v19.

Muñoz-Sabater, J., E. Dutra, A. Agustí-Panareda, C. Albergel, G. Arduini, G. Balsamo, S. Boussetta, M. Choulga, S. Harrigan, H. Hersbach, B. Martens, D. G. Miralles, M. Piles, N. J. Rodríguez-Fernández, E. Zsoter, C. Buontempo, and J.-N. Thépaut (2021). ERA5-Land: A State-of-the-Art Global Reanalysis Dataset for Land Applications. *Earth System Science Data* 13, pp. 4349–4383. https://doi.org/10.5194/essd-13-4349-2021.

Nairn, J. R. and R. J. B. Fawcett (2015). The Excess Heat Factor: A Metric for Heatwave Intensity and Its Use in Classifying Heatwave Severity. *International Journal of Environmental Research and Public Health* 12.1, pp. 227–253. https://doi.org/10.3390/ijerph120100227.

Statistics Mauritius (2022). *2022 Population Census, Volume III: Geographical and Migration Characteristics, Table G1: Resident Population by Geographical Location, Whereabouts on Census Night and Sex*. Government of Mauritius. Final table report; Island of Mauritius resident population 1,189,493.

Stull, R. (2011). Wet-Bulb Temperature from Relative Humidity and Air Temperature. *Journal of Applied Meteorology and Climatology* 50.11, pp. 2267–2269. https://doi.org/10.1175/JAMC-D-11-0143.1.

Tartarini, F. and S. Schiavon (2020). pythermalcomfort: A Python Package for Thermal Comfort Research. *SoftwareX* 12, p. 100578. https://doi.org/10.1016/j.softx.2020.100578.

World Meteorological Organization (2026). *Extreme Heat*. WMO thematic overview of extreme-heat definitions, monitoring, impacts and early-warning response. URL: `https://wmo.int/themes/extreme-heat` (visited on 09/24/2026).

World Meteorological Organization and World Health Organization (2015). *Heatwaves and Health: Guidance on Warning-System Development*. WMO-No. 1142. Geneva, Switzerland: World Meteorological Organization. ISBN: 978-92-63-11142-5.